International Journal of Mining Science and Technology 26 (2016) 149–154

Contents lists available at ScienceDirect

International Journal of Mining Science and Technology

journal homepage: www.elsevier.com/locate/ijmst

# Determination of volumetric changes at an underground stone mine: a photogrammetry case study

Slaker Brent [a,*], Westman Erik [a], Ellenberger John [b], Murphy Michael [b]

[a] Virginia Polytechnic Institute and State University, Blacksburg 24060, USA
[b] Office of Mine Safety and Health Research, NIOSH, Pittsburgh, PA 15236, USA

ARTICLE INFO

*Article history:*
Received 30 July 2015
Received in revised form 8 October 2015
Accepted 27 October 2015
Available online 28 December 2015

*Keywords:*
Photogrammetry
Limestone
Underground mining
Displacement
Monitoring

ABSTRACT

Photogrammetry, as a tool for monitoring underground mine deformation, is an alternative to traditional point measurement devices, and may be capable of accurate measurements in situations where technologies such as laser scanning are unsuited, undesired, or cost-prohibitive. An underground limestone mine in Ohio is used as a test case for monitoring of structurally unstable pillars. Seven pillars were photographed over in a 63 day period, punctuated by four visits. Using photogrammetry, point clouds of the mine geometry were obtained and triangulation surfaces were generated to determine volumes of change over time. Pillar spalling in the range of 0.29–4.03 $m^3$ of rock on individual rib faces was detected. Isolated incidents of rock expansion prior to failure, and the isolated failure of a weak shale band were also observed. Much of the pillars remained unchanged during the monitoring period, which is indicative of proper alignment in the triangulated surfaces. The photographs of some ribs were of either too poor quality or had insufficient overlap, and were not included. However, photogrammetry was successfully applied to multiple ribs in quantifying the pillar geometry change over time.



## 1. Introduction

Adequately measuring underground rock mass movements is integral to understanding how rock masses behave and how to interact with them safely and efficiently. Many modern measurement techniques employed in underground mining environments rely on point measurements, such as through extensometers or borehole relief methods [1]. These techniques, while commonplace, do not provide a comprehensive view of how the rock mass is behaving. The dynamic changes in stress states underground, coupled with the mechanical uncertainty of rock masses, near active excavations, creates a need for measurement systems which better capture the true behavior of the rock mass. Laser scanning and photogrammetry are two such measurement technologies that provide wide-area monitoring capabilities.

Digital photogrammetry will be tested in this study, not because of its superiority, but due to its more probable adoption in hazardous mining environments. Digital photogrammetry is a means of obtaining three-dimensional point clouds from digital photographs. Close range digital photogrammetry (CRDP) is photogrammetry applied to measuring objects or scenes less than 100 m away, and is used for various functions in underground mining environments [2]. These uses include, but are not limited to mapping fracture networks, characterizing fractures, and measuring volumes of blast rock [3–6].

One additional application to underground mining environments is monitoring geometric change in support structures, such as pillars. Using time-lapse observations, three-dimensional point clouds or surfaces can be compared to observe temporal change. The ability to measure or observe object displacements in an underground mining setting, using photogrammetry, differs in practice and obstacles from a surface setting. This study explores the viability of applying photogrammetry to monitoring temporal geometric change in pillar structures.

### 1.1. Site description

The setting for this study is an underground limestone mine in eastern Ohio. The mine follows the Vanport Limestone seam, with a mining depth that ranges from 60 to 75 m, while maintaining a near-horizontal inclination. The mine plan consists of varying pillar sizes and orientations, with many pillars reduced from their planned size due to over mining and scaling or sloughing. The predominant planned pillar dimension was 7.6 m wide and 18.2 m long, on 30 m crosscut centers and 19.8 m drift centers. This results

* Corresponding author. Tel.: +1 757 8803050.
*E-mail address:* slakerba@gmail.com (B. Slaker).

http://dx.doi.org/10.1016/j.ijmst.2015.11.023
2095-2686/

in the north–south crosscuts that are 12 m wide with the east–west crosscuts also being 12 m wide.

The mine has experienced significant structural instabilities. A collapse on May 27th, 2014 encompassed 10 pillars in a 61 m by 107 m region, and an additional collapse, involving 10 pillars, occurred on June 24th, 2014. Spalling and scaling of pillars occurred throughout the mine, and when coupled with over mining, resulted in pillar dimensions likely in the range of 6.4 m by 17.0 m, instead of the planned 7.6 m by 18.2 m.

The instability is believed to be due to the presence of weak 20–30 cm shale bands within the pillar and a weak 1 m thick moisture-sensitive fireclay beneath the pillar. The weak bands can create tension in the surrounding strata through extrusion, and if the pillars punch into the weak floor strata, it can create floor heave and reduce the support provided to the roof. Further detail of site characterization and mechanisms of the pillar failures are discussed by Murphy et al. [7]. The collapse of roof structures is beyond the scope of this study, but the sloughing and scaling associated with this instability provides an excellent subject for photogrammetry.

## 2. Methods

Seven pillars were photographed across four different visits: August 26th, September 16th, September 26th, and October 28th 2014. The photographs were taken with a Digital Single-Lens Reflex (DSLR) Nikon D70S camera. Camera settings, shown in Table 1, were kept consistent during visits, but slight changes were made between them. The lighting was provided by a source external to the camera, which was moved as needed to provide sufficient light on the subject. The photographs were taken by hand, without the aid of a tripod. Several photographs were of poor quality, but were still used for reconstruction if clearer photographs were unavailable. Fog is believed to be partially responsible for blur in some photographs, as well as a lower *f*-number causing spherical aberration in the lens.

**Table 1**
Photograph EXIF data from each visit.

| Date | Resolution | *f*-number | Shutter speed (s) | Focal length (mm) |
|---|---|---|---|---|
| Aug. 26th | 3008 × 2000 | *f*/2.8 | 1/80 | 20 |
| Sep. 16th | 3008 × 2000 | *f*/2.8 | 1/80 | 20 |
| Sep. 26th | 3008 × 2000 | *f*/2.8 | 1/60 | 20 |
| Oct. 28th | 3008 × 2000 | *f*/4.5 | 1/60 | 20 |

A map of the pillars that were photographed is shown in Fig. 1. The pillars are on the boundary of a collapsed area. The number of photographs taken of each pillar is listed in Table 2. With the need to move the light sources, the pictures were not taken continuously surrounding the pillar, but rather in distinct segments, fragmenting the pillar into "sides" instead of one contiguous object. Further displacement of material, through spalling, on these pillars was expected, but the magnitude of material being displaced was unknown.

The photographs were processed through a combination of Agisoft Photoscan, CloudCompare, and Maptek iSite. Photoscan was used to obtain the point clouds and triangulation surfaces from the photographs. Next, CloudCompare was used to orient and scale the time-lapse photos. Several 30 cm squares were placed in each scene to provide a reference for scaling the resultant triangulation surfaces. The squares were not placed in the same location during subsequent visits, and as a result, would create the appearance of movement on the rib face at the locations they were placed.

Orienting the photos was performed by locating the same points on the rib or roof between visits. Exposed rock faces have a significant number of visual features that can be located across the photographs from different visits and assigned the same three-dimensional coordinate. Four of these features were chosen in each point cloud to align with a point cloud of the same region at the next visit. If reference points moved between scenes, such as in the expansion of a rib, this would cause a systematic error clearly visible when aligning the triangulation surfaces.

Lastly, iSite was used to determine the distances between the triangulation surfaces at different time periods. The volumes reported are the volumes enclosed by two triangulation surfaces. The older surface will always be the reference. Negative volumes correspond to the removal of material from the rib, while positive volumes correspond to an expansion of the rib or accumulation of material that did not previously exist. The same process was applied previously, in an underground limestone mine, using laser scanning as the point cloud collection method [8].

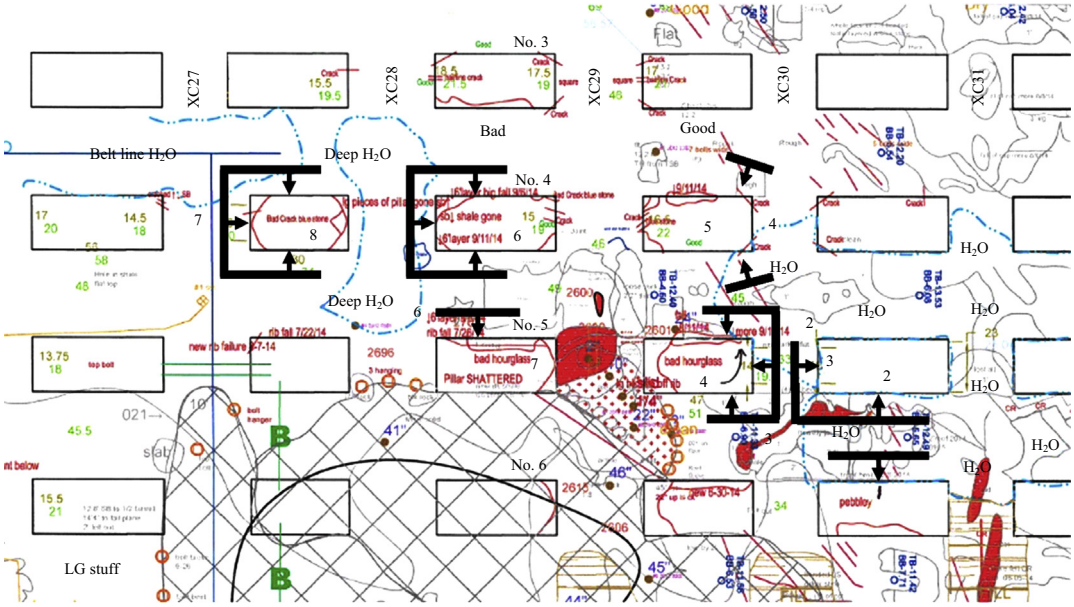


**Fig. 1.** Map of the photographed areas of the mine with pillars numbered.

**Table 2**
Number of pictures taken at each pillar.

| Pillar | Aug. 26 | Sep. 16 | Sep. 26 | Oct. 28 |
|---|---|---|---|---|
| 1 | 0 | 03 | 05 | 0 |
| 2 | 0 | 11 | 07 | 2 |
| 3 | 05 | 09 | 08 | 6 |
| 4 | 00 | 04 | 11 | 7 |
| 5 | 02 | 13 | 11 | 5 |
| 6 | 04 | 05 | 0 | 0 |
| 7 | 12 | 09 | 0 | 3 |

These software packages are not uniquely able to perform these functions, nor are the software packages limited in use to the function presented here. The reason for using each was the preference of the author. Due to the poor quality of some photographs, a significant cascading error may exist in some of the point clouds. Imprecisely constructed point clouds can lead to imprecise scaling and inaccurate referencing, resulting in underestimations or overestimations of volume change. Point clouds, which appears to be significantly noisier than the rest, are noted in their relevant section.

## 3. Results

The time-lapse analysis of surface change, as calculated by iSite, is shown in Figs. 2–9. The colored surface has been overlain on a photograph of the scene at the earlier time in the analysis. The overlain pictures are approximately aligned by hand; however, the volumes of change are calculated by iSite from the two referenced surfaces.

The change observed at pillar 1, in Fig. 2, is likely to be artifacts of the photogrammetry. The Sep. 16th pictures were both blurry and in very low light, resulting in a questionable point cloud. The presence of localized expansion of the magnitude being shown

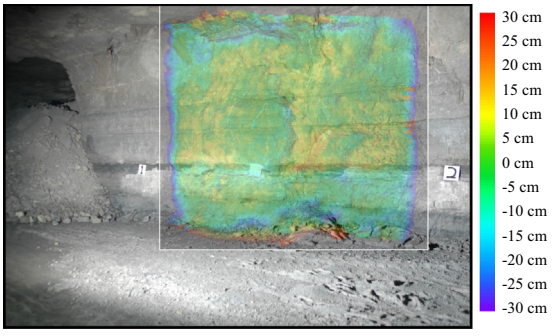


**Fig. 2.** Change at pillar 1 between Sep. 16th and Sep. 26th.

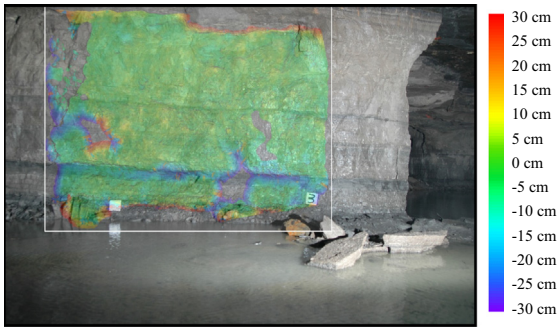


**Fig. 3.** Change at pillar 2 between Sep. 16th and Sep. 26th.

should result in visible tension cracks when comparing the photos, but no such cracks exist.

The change in pillar 2, on the side shown in Fig. 3, is confined to the weak shale band nearest to the base of the pillar. The uniform absence of deformation elsewhere, combined with the spalling of material from this band, follows the behavior suggested by Murphy et al. [7]. The holes in the overlay at the left-center and bottom-center do not indicate that large portions of the rib changed between photographs, but were merely areas that were unable to be reconstructed.

The other visible side of pillar 2, shown in Fig. 4, exhibited little to no deformation between Sep. 16th and Sep. 26th, with the exception of the references placed on the rib, however, a large change in the rib was detected sometime between September 26th and October 28th. The area highlighted in Box A showed 0.36 $m^3$ of change between the time periods. The change was likely larger than this, but the reconstructed area of pillar 2 for the second time period was smaller than the first due to insufficient overlap between pictures.

Three sides of pillar 3 were photographed. The first side, Fig. 5, shows widespread removal of material along the left side in the Aug. 26th to Sep. 26th time frame, however, there were only two photographs in the first set (Aug. 26th), and both were blurry. The widespread change cannot be verified in the pictures due to the image quality, with the exception of the dark blue area near the center where a change does appear to have occurred. A clear change is visible in the Sep. 26th to Oct. 28th time frame, with the area enclosed by Box A showing a displacement of 0.52 $m^3$.

Both time periods at pillar 3 in Fig. 6 shows a small amount of movement on the right side of the pillar, with a crack clearly visible by Sep. 26th, which separates the moving region of the rib from the stationary region. The areas inside Box A and Box B also show rather small, but distinct displacement. The change shown in Box A for the Sep. 26th to Oct. 28th time period shows 0.29 $m^3$ of change, however, this occurs in an area with pronounced shadows which may be affecting the results. The rest of the pillar face is free of shadows and shows no significant change.

Fig. 7 shows the last side of pillar 3, which includes numerous pockets of change between Sep. 16th and Sep. 26th. This is most likely due to shadows, which were significantly pronounced in one of the two photos from September 16th. The Sep. 26th to Oct. 28th time period does not include the shadowed photographs and shows far fewer, but verifiable, pockets of change, although no large rib movements.

The first time period, from Sep. 16th to Sep. 26th, in Fig. 8, shows no significant movement, with the small color variations likely due to the poor quality of the photographs used. The second time period, from Sep. 26th to Oct. 26th, a large displacement of rib material was detected. In the area enclosed by Box A, 4.03 $m^3$ was displaced. The other sides of this pillar were inaccessible when the next visit occurred on Oct. 28th.

It is difficult to verify the change present in Fig. 9, due to the blurriness of the photographs. Change does appear to have occurred in the area enclosed by Box A, however Box B and Box C are inconclusive. A photograph of this area was taken on Sept. 26th, and it showed significant damage across the rib face, possibly a result of the movement shown taking place between Aug. 26th and Sep. 16th. In addition to the pillars shown, observations at the remaining photographed pillars are summarized in Table 3.

The pillar behaviors observed can be classified into four categories: spalling, expansion, weak band failure, and no movement. Nearly all the pillars exhibited spalling, which is shown on pillars 2, 3, 5, 6, and 7. This spalling ranges from 0.29 to 0.52 $m^3$ of material being displaced from the rib. The spalling behavior shown on pillar 2 and 3 occurred at the corner of the pillar and was poorly quantified as a result. Due to the light positioning, another set of

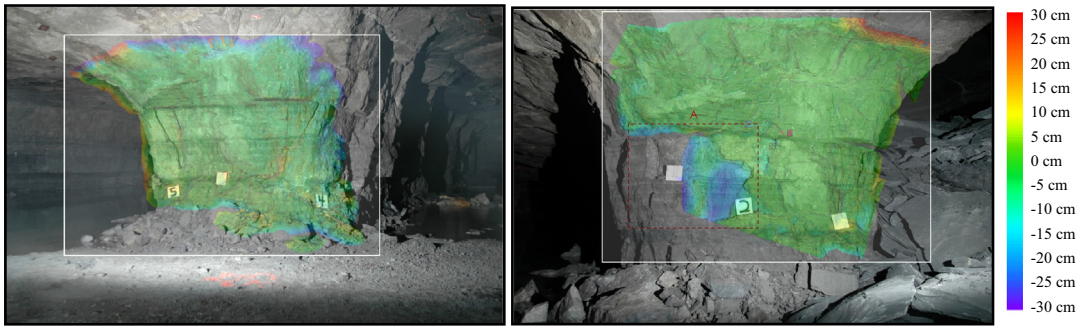


**Fig. 4.** Change at pillar 2 from Sep. 16th to Sep. 26th (top) and Sep. 26th to Oct. 28th (bottom).

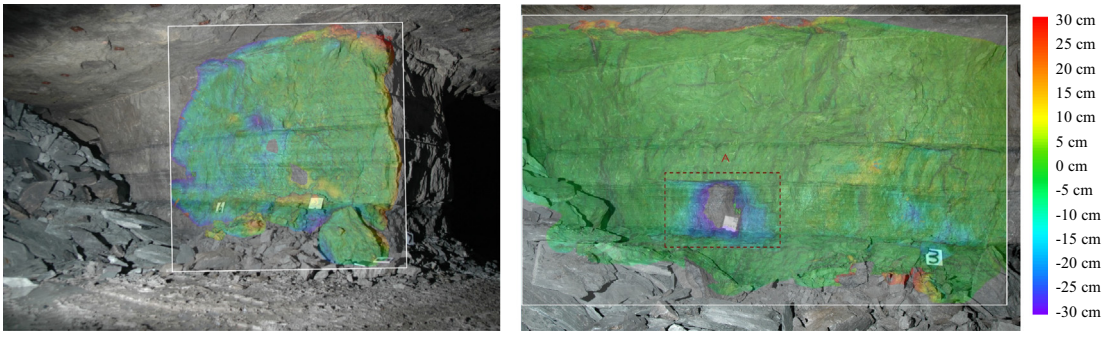


**Fig. 5.** Change at pillar 3 from Aug. 26th to Sep. 26th (top) and Sep. 26th to Oct. 28th (bottom).

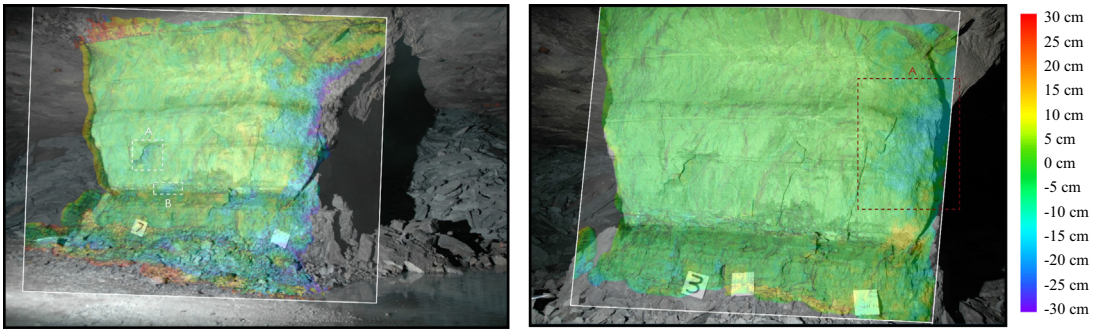


**Fig. 6.** Change at pillar 3 from Aug. 26th to Sep. 26th (top) and Sep. 26th to Oct. 28th (bottom).

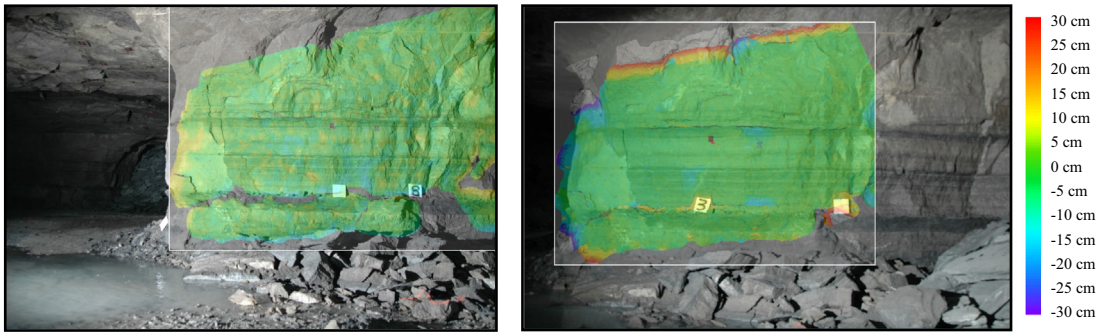


**Fig. 7.** Change at pillar 3 from Sep. 16th to Sep. 26th (top) and Sep. 26th to Oct. 28th (bottom).

photos would need to be taken solely of the pillar corner in order to reconstruct it properly. Photographs were not taken of the corner, but instead each side of the pillar was reconstructed, leaving the corner deformation quantitatively unknown. Pillars 3, 5, 6, and 7 all showed some degree of spalling away from the corners, although the 4.03 $m^3$ displaced on pillar 5 was the largest by far. This spalling did not appear preferentially located at certain parts of the rib.

Expansion, or an observed movement of the rib towards the camera, was shown on several pillars, but this could also be

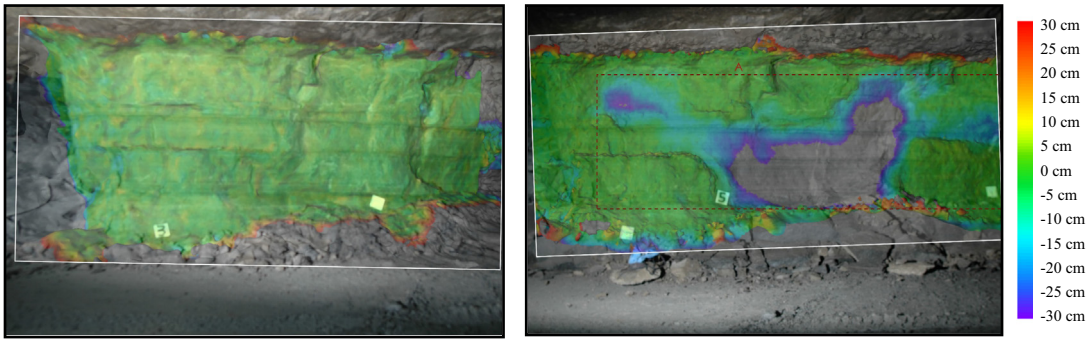


**Fig. 8.** Change at pillar 5 from Sep. 16th to Sep. 26th (top) and Sep. 26th to Oct. 28th (bottom).

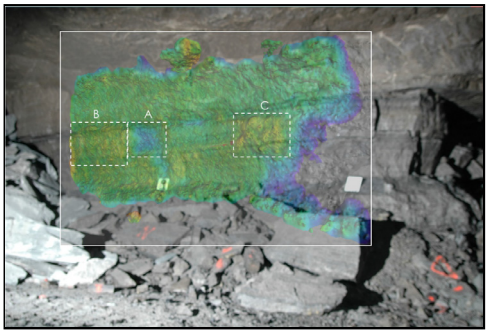


**Fig. 9.** Change at pillar 6 from Aug. 26th to Sep. 16th.

**Table 3**
Summary of conditions at each pillar.

| Pillar | Condition | Note |
|---|---|---|
| 1 | An example of a poorly aligned point cloud | Blurriness negatively impacted the reconstruction of the Aug 26th to Sep. 16th time period |
| 2 | A large part of the corner of the rib was displaced, and there was significant displacement in the weak shale band | Overlapping between photographs was not high enough to capture fully the displacement |
| 3 | An isolated 0.52 $m^3$ displacement occurred | Blurriness negatively influenced the reconstruction of the Aug 26th to Sep. 16th time period |
| 4 | Good | No detectable change occurred during the monitoring period |
| 5 | A large 4.03 $m^3$ displacement occurred | Two sides of the pillar were inaccessible following the displacement between Sep. 16th and Oct. 28th |
| 6 | Small areas of localized rib spalling and rib expansion are detected | Photographs from Oct. 28th show significant damage in the areas that were expanding, but the photographs were blurred |
| 7 | Significant rib spalling occurred between Aug. 26th and Sep. 16th, but none after that time period | The Aug. 26th and Sep. 16th photographs were blurry, but less pronounced than at Pillars 1 and 3. Fog may have played a role in reducing the quality of these photographs |

indicative of a poorly aligned or reconstructed point cloud. Considering the photographic quality at each site, pillar 6 is the only likely candidate for showing actual expansion of the rib. A photograph that was taken on the visit following the observed expansion shows significant damage in one of the expanding areas. That photograph showed no change in the area that had already shed material. With the uncertainty associated with the photographs, this is not conclusive, but is potentially predictive of areas that would experience failure.

A weak shale band near the base of the pillar showed distinct spalling on one side of pillar 2. Large displacements were confined to this band. The short sides of the pillar did not show the same displacement in this band. No other pillars showed widespread failure of this shale band.

Many of the pillars also show no movement at all, or the majority of their surface area is left unchanged between observation periods. An unchanging rib face makes quantification of rib displacement inapplicable, but it does demonstrate the reliability of that surface's orientation. Properly oriented triangulation surfaces will show zero movement if none occurred, and any reported change in geometry must be a result of material movement or disruptive photographic elements, such as moving reference targets.

## 4. Conclusions

An Ohio limestone mine experienced large roof falls due to structural instabilities caused by weak strata bands. The structural problems were evident in the pillar geometry as varying amounts of material spalled, or were scaled, from the pillars. The change in pillar geometry over time was monitored at seven different pillars using photogrammetry. The photographs were taken at four separate dates: Aug. 26th, Sep. 16th, Sep. 26th, and Oct. 28th, 2014. Not all pillars were photographed at each date, and nor were all photographs of the same quality, although efforts were taken to keep camera settings consistent throughout an entire visit.

Four different pillar behaviors were observed during this monitoring period: weak band failure, spalling or scaling, expansion, and no movement. The weak band failure was observed in one pillar, with a weak shale band approximately 20–30 cm in width losing material between Sep. 16th and Sep. 26th. Any subsequent structural issues the band failure may have caused were not observed between those two dates.

Spalling or scaling was observed on four pillars, with three being relatively small amounts of material, 0.29–0.52 $m^3$, displaced between monitoring periods. Another pillar showed significantly more material, 4.03 $m^3$, displaced between monitoring periods.

One pillar face showed a small amount of spalling while simultaneously showing other areas of expansion. The expansion was generally less than 15 cm, but the quality of the photographs was not high enough to locate clear tension cracking as a result. The picture following the expansion between Aug. 26th and Sep. 16th, on Sep. 26th showed significant damage in the areas that had been expanding. This damage would be expected if the pillar was inelastically expanding.

Some pillars experienced either no movement or very little movement across the monitoring period. Just as it is important to be able to detect material movement, it is also important to be able to detect the absence of movement, and not suggest that

structural instabilities exist where they do not. Several triangulated surfaces do show false movements between time periods, but these generally show anomalies across the entire surface, and are a result of a poor photogrammetric reconstruction.

The time-lapse photogrammetric monitoring performed at this site resulted in seven pillars being successfully reconstructed. The precision of measurements varied with photograph quality, but expected rib changes were modeled and capable of being quantified. Remote sensing has been shown to be uniquely suited for measurement of large mine areas, and can offer a supplementary perspective on the mine behavior of which traditional point measurement techniques may be incapable.

## References

[1] Christiansson R. The latest development for in-situ rock stress measuring techniques. In: Proceedings of the international symposium on in-situ rock stress. Trondheim, Norway; 2006. p. 3–10.

[2] Atkinson KB. Close range photogrammetry and machine vision. Dunbeath, Caithness, Scotland: Whittles Publish; 1996.

[3] Kim J, Kim D, Won K. Measurement of joint orientations of tunnel working face using a new photogrammetric technique. In: Proceedings of the 40th US symposium on rock mechanics; 2005.

[4] Petteri Somervuori ML. Modern 3D photogrammetry method for rock mechanics. Geological mapping 3D model and documentation of open pit faces and tunnels; 2010.

[5] Styles T, Zhang Y, Stead D, Elmo D, Roberts D, Yanske T. A photogrammetric approach to brittle fracture characterization in mine pillars. In: Proceedings of 44th US rock mechanics symposium and 5th US–Canada rock mechanics symposium, Lake City; 2010.

[6] Heal D, Hudyma M, Potvin Y. Assessing the in-situ performance of ground support systems subjected to dynamic loading. In: Proceedings of Ground support in mining and underground construction, the 15th international symposium on ground support. Perth, Australia; 2004. p. 28–30.

[7] Murphy M, Ellenberger J, Esterhuizen G, Miller T. Roof and pillar failure associated with weak floor at a Limestone mine. In: Proceedings of 2015 SME annual meeting & exhibit; 2015.

[8] Slaker B, Westman E, Fahrman B, Luxbacher M. Determination of volumetric changes from laser scanning at an underground limestone mine. Min Eng 2013;65:11.